

SOFT BIOMETRIC TRAIT ON FINGERVEIN RECOGNITION USING CNNRESNET

N Nibishaa*¹, SV Brindha*²

*^{1,2}Department Of Electronics And Communication Engineering, Vins Christian College Of Engineering, Tamil Nadu, India.

DOI : <https://www.doi.org/10.56726/IRJMETS45027>

ABSTRACT

Numerous algorithms for finger vein feature extraction demonstrate commendable performance by emphasizing texture characteristics, yet some overlook the intensity distribution of the finger tissue, treating it as background noise in certain instances. Use this kind of noise as a novel soft biometric feature in this project to achieve better output in finger vein recognition. To begin, a thorough examination of the finger vein imaging theory and image characteristics is presented, showcasing the potential extraction of the intensity distribution generated by the finger tissue background for identification as a soft biometric feature. Subsequently, this study introduces two algorithms for extracting the background layer of finger vein patterns and three algorithms for extracting soft biometric traits from the intensity distribution. In the classification stage developed a system with implementation of convolution neural network specifically RESNET18 for the training image dataset and image retrieving process is done. Purpose of introducing deep learning in developing finger vein identification system is to get accurate more performance and speedy results. These are computed on the basis Euclidean distance between features obtained from test image and features of trained images, the model designed has good robustness in illumination and rotation.

Keywords: Finger vein, Soft Biometric, Extraction, Intensity Distribution, RESNET18, Convolution Neural Network.

I. INTRODUCTION

In response to the heightened demands for authentication, traditional authentication technologies are falling short of meeting the requirements of the present era. In comparison to conventional authentication methods such as keys, cards, and passwords, biometric technology emerges as a more potent guardian of personal identity information, boasting significantly improved security and effectiveness. Recently, finger vein biometric technology has captured the attention of numerous research groups, revealing substantial market potential. Finger vein patterns, situated within the human body with their inherent biological activity, pose an almost insurmountable barrier to replication. Relative to other biometric technologies, finger vein recognition offers distinctive advantages: firstly, it hinges on an individual's unchanging internal characteristic, ensuring a high degree of uniqueness and stability over time. Secondly, the need to capture finger vein images from a living body makes them exceptionally resistant to forgery, theft, or environmental influences like skin conditions, pollution, and temperature. Thirdly, the compact, non-contact nature of finger vein collection devices enhances user acceptability and friendliness. However, traditional finger vein recognition algorithms encounter limitations that can curtail their broader applications. These algorithms traditionally rely on manually crafted approaches for feature extraction, often categorized as local binary-based and vein pattern-based methods. Unfortunately, these techniques may introduce irregular shadows and lead to the loss of essential vein feature image information, resulting in diminished matching accuracy. Moreover, traditional methods involve complex steps to learn a feature transformation matrix, necessitating retraining when incorporating new users, constraining the recognition potential of the model. Furthermore, certain traditional finger vein recognition algorithms necessitate specific sensors during the finger vein image acquisition process, limiting their generalizability.

To address these limitations, deep convolutional neural networks (CNNs) have emerged as a transformative approach. These networks utilize convolution kernels of varying sizes to comprehensively extract finger vein image features, ensuring a detailed representation. The use of lightweight CNN structures not only accelerates vein recognition but also preserves matching accuracy. Some neural network-based finger vein recognition

algorithms have demonstrated superior performance compared to their traditional counterparts in terms of accuracy. Additionally, deep learning methods allow for the replacement of manually extracted features with unsupervised or semi-supervised feature learning. Similar to face recognition, finger vein recognition involves selecting regions of interest with distinctive vein features, followed by feature extraction and matching. However, there is a scarcity of publicly available finger vein datasets suitable for training deep models. Furthermore, some deep networks, such as Google-Net and ResNet, face challenges in achieving real-time finger vein matching due to an excessive number of parameters.

In addressing these challenges, novel and inventive methodologies have surfaced. One approach integrates the fully convolutional neural network with conditional random fields to achieve precise vein pattern segmentation. Another method employs a lightweight real-time segmentation algorithm for finger veins, enhancing matching efficiency, albeit with room for improvement in detection accuracy. A multi-receptive field bilinear convolutional neural network has also been utilized for finger vein recognition, enhancing accuracy while reducing training time and model parameters. A lightweight convolutional neural network, incorporating triplet loss for finger vein recognition, employs a multi-scale approach for initial feature extraction and gradually acquires detailed features, resulting in improved matching accuracy with reduced computational effort. Importantly, this approach allows for the identification of new categories by calculating spatial vector distances, thereby avoiding repetitive training.

The system for personal identification based on finger vein patterns comprises three fundamental modules: image acquisition, preprocessing, and matching. During image acquisition, a finger is appropriately illuminated by a near-infrared (NIR) light source from above, and the camera situated below captures the finger vein image. This setup exploits the differential absorption of NIR light by hemoglobin in the finger veins, resulting in darker vein areas and lighter surrounding tissue in the captured image. The integrity of the finger vein pattern significantly influences the recognition rate. However, issues like overexposure and underexposure can lead to information loss, often irrecoverable through image enhancement techniques. Therefore, it becomes imperative to regulate the illuminance distribution during the image acquisition process to mitigate overexposure and underexposure. This adjustment ensures that the acquired finger vein image retains the maximum possible information about the finger vein pattern.

This article makes the following key contributions.

- A swift and precise finger vein feature extraction and recognition algorithm founded on a lightweight deep convolutional neural network. This approach surpasses existing depth model algorithms in terms of recognition accuracy and matching efficiency.
- The utilization of a triplet loss function during the deep model training process. This loss function proves highly effective in extracting and recognizing features from fine-grained images, while also facilitating the construction of a 3-D vector space for finger veins. This, in turn, eliminates the need for multiple rounds of model training.
- The introduction of a maximum curvature finger vein pattern feature extraction and optimization algorithm, incorporating Gaussian filtering optimization. This novel method excels in extracting pattern features from finger veins and mitigates the impact of noise on recognition accuracy.

II. LITERATURE REVIEW

In this article, Shun-Chi, et al. presents an ECG-based biometric recognition system aimed at enhancing IoT-driven patient monitoring security. Focusing on identification mode, they employ "subspace oversampling" to create unique templates for enrollees, ensuring privacy and preventing cross-matching. "Subspace matching" enables identity determination from beat bundles without additional template data. The system also includes a mechanism for excluding unregistered subjects, further bolstering security. Evaluation with 287 subjects yielded a low linkability rate of 0.0938, a 99.02% identification rate, and a 0.44% false-positive identification error rate, even under dictionary attack scenarios with real ECG data.

Sengupta, et al. introduce a novel method to enhance hardware accelerator security against ownership threats by employing biometric fingerprinting. They convert the IP vendor's biometric fingerprint into digital templates, embedding them as secret constraints within the accelerator design. Key findings include

remarkably low probabilities of coincidence (P_c) ranging from $2.22E-3$ to $4.35E-6$ for 11 different fingerprints. Additionally, resource constraints have negligible design cost overhead (0%) for JPEG compression hardware. Comparative analysis demonstrates that their biometric fingerprinting approach achieves P_c values $3.9E+2$ to $6.9E+4$ times lower than recent work, substantially improving hardware accelerator security.

Qian, et al. introduced MuDeep, a novel deep re-identification (re-id) network featuring two innovative layer types: a multi-scale deep learning layer and a leader-based attention learning layer. The former facilitates the acquisition of deep discriminative features at various scales, while the latter harnesses multi-scale information to guide and determine optimal weightings for each scale. MuDeep explicitly learns the significance of different spatial locations for feature extraction through its leader-based attention learning layer. Extensive experiments demonstrated MuDeep's superiority over existing methods across multiple benchmarks, particularly excelling in domain generalization scenarios.

Yang, et al. introduced the Finger-Vein Recognition and AntiSpoofing Network (FVRAS-Net), a lightweight convolutional neural network (CNN) that unifies recognition and antispoofing tasks via multitask learning (MTL). This integrated model delivers high security and real-time performance. Furthermore, they implemented a multi-intensity illumination strategy within the biometric system, automatically selecting the most informative finger-vein image for identification, significantly enhancing real-system recognition. Experimental results on public datasets, including challenging ones with axial rotation images, demonstrate FVRAS-Net's outstanding performance in both recognition and antispoofing tasks.

Finger-vein biometric recognition has gained attention for its resilience against attacks and user-friendly approach. Commercial systems exist but often demand users to keep their hand still for a few seconds during recognition. In this study, Kuzu, et al. aim to remove this constraint by enabling on-the-fly finger vein pattern acquisition. They introduce a dedicated acquisition setup using low-cost cameras and propose a recognition framework combining Convolutional and Recurrent Neural Networks. Experimentation involving a dataset of finger vein videos with varying exposure times from 100 subjects demonstrates remarkable performance, with recognition accuracy reaching up to 99.13% in a challenging setting.

In finger vein verification, the challenge is robust vein pattern extraction from low-contrast infrared images. Recent CNN-based methods face image size constraints and issues with ground-truth pattern maps quality due to outliers and vessel disruptions. Addressing these, Chen, et al. introduces FV-GAN, leveraging generative adversarial networks (GANs). Unlike traditional CNNs, FV-GAN learns from the joint distribution of finger vein images and pattern maps for enhanced robustness. It adopts fully convolutional networks, eliminating fully connected layers to accommodate various image sizes and reduce computational costs. Experimental results on two databases demonstrate FV-GAN's substantial improvement in verification accuracy and equal error rates.

Liu, et al. introduces a novel method, Category-Preserving Binary Feature Learning and Binary Codebook Learning (CPBFL-BCL), for finger vein recognition. This approach emphasizes discrimination in learned binary features by incorporating Fisher discriminant analysis and category manifold preservation during the feature learning process. Additionally, it employs a unique binary clustering technique based on K-means clustering to generate a binary codebook. Experimental results, conducted on two public finger vein databases, showcase the efficacy and efficiency of this method. It outperforms existing finger vein techniques and a finger vein retrieval method in both recognition and retrieval tasks.

ADVIT, a novel identification tool proposed by Hussain et al., utilizes dorsum vein patterns for human identification, addressing manual feature calculation challenges. The study, involving 50 participants, preprocesses hand images to extract vein skeletons and generate binary vein pattern images. By merging hand-crafted grid-based features with deep representations from RESNET-50, the model achieves high accuracy (0.8861) and sensitivity (0.8803), offering potential assistance to forensic scientists in perpetrator identification.

III. PROPOSED SYSTEM

Introducing CNNRESNET, a novel solution for soft biometric trait recognition in finger vein authentication. This innovative approach leverages a lightweight deep convolutional neural network to develop a fast and accurate finger vein feature extraction and recognition algorithm, outperforming existing depth model algorithms in

both recognition accuracy and matching efficiency. The block diagram of the finger vein recognition system framework combining a primary biometric trait and the proposed soft biometric trait is depicted in Fig. 1.

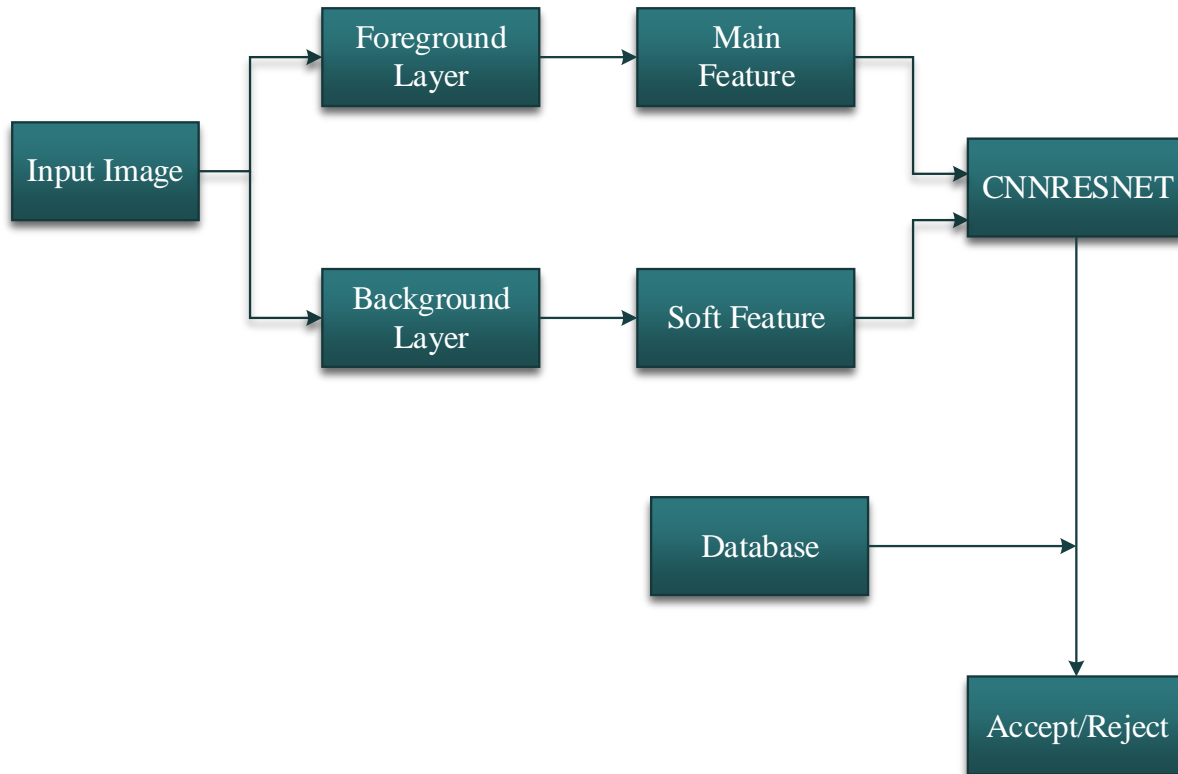


Figure.1. Block Diagram of Proposed System

In this approach, the input image is initially separated into two distinct layers: the foreground layer and the background layer, accomplished through a novel "image layer separation" technique. Subsequently, the primary biometric trait is extracted from the foreground layer, while the soft biometric trait is derived from the background layer using various methods. Authentication of an individual's identity is then conducted using an artificial neural network, effectively classifying pixels within any region of a test image. An innovative soft biometric trait is introduced to enhance finger vein recognition performance, specifically focusing on the intensity distribution within the finger vein image background. Notably, this marks the first exploration of intensity distribution as a soft biometric trait in finger vein recognition.

The method effectively extracts the intensity distribution as a soft biometric trait. Given that a finger vein image comprises both the foreground layer (containing texture information) and the background layer (containing intensity distribution information), the approach begins by employing a background layer extraction algorithm to isolate the intensity distribution. Subsequently, the intensity distribution is described in three distinct ways. During the classification stage, a convolutional neural network, particularly ResNet, is employed for training on the image dataset and performing image retrieval. The introduction of deep learning in the finger vein identification system aims to achieve enhanced accuracy, improved performance, and faster results.

3.1. PREPROCESSING

The initial preprocessing step involves resizing images to their required dimensions, ensuring they match the desired scale without altering pixel information. Image resizing results in an image that is SCALE times the size of the input image. Another critical technique is histogram equalization, which enhances image contrast by redistributing intensity values, effectively stretching the intensity range. This process generally boosts global contrast, particularly benefiting regions with initially close contrast values, thereby improving overall image quality.

3.2. IMAGE LAYER SEPARATION

The foreground layer comprises the texture information, while the background layer contains intensity

distribution details. Gaussian blur (GB) emerges as a natural approach for obtaining the background layer. This is because finger vein texture can be seen as high-frequency components, whereas the background's intensity distribution corresponds to low-frequency components. GB serves as an effective low-pass filter, effectively eliminating the finger vein texture and retaining only the background layer.

3.3. FEATURE EXTRACTION

Feature extraction serves as a dimensionality reduction technique, effectively condensing significant aspects of an image into a concise feature vector. This method proves valuable, especially when handling large image sizes and necessitating a streamlined feature representation for expeditious task execution, such as image matching and retrieval. Given the distinct structural variations among different fingers, encompassing factors like knuckle position, bone structure, finger thickness, and tissue water content, the intensity distributions of various finger veins exhibit disparities in transmitted imaging a prevalent method employed for finger vein image acquisition.

3.3.1. Primary Biometric Trait Extraction

The foremost biometric trait holds paramount significance as it plays a pivotal role in ensuring the system's accuracy. LBP, an efficient texture extraction algorithm renowned for its illumination and rotation invariance, is commonly employed in vein recognition. The fundamental concept behind LBP entails quantifying the grayscale variation between each pixel and its local vicinity, encoding this variation to produce the LBP code histogram an all-encompassing representation of the finger vein feature.

3.3.2. Soft Biometric Trait Extraction

Individuals' background layers exhibit varying intensity distributions, a crucial aspect for soft biometric trait extraction. We have devised three key soft biometric traits derived from the background layer diversity.

Incorporating these three key soft biometric traits derived from background layer diversity significantly enhances our finger vein recognition model's discrimination capabilities. The mean and variance measurements provide valuable insights into global brightness and contrast variations across backgrounds, offering a solid foundation for accurate identification. Extending the analysis to an array of mean and variance values enables us to capture localized intensity distribution variations, making our system more robust in complex scenarios. Additionally, our multi-scale approach through the Histogram of Spatial Pyramid dissects intensity distribution hierarchically, providing nuanced insights that further bolster our model's accuracy in user identification. Together, these traits form a comprehensive toolkit that ensures reliable and precise recognition, even in challenging real-world conditions.

3.3.3 Mean and Variance

The uniqueness of individuals' fingers lies in the subtle variations in both thickness and tissue density. These physical attributes manifest themselves vividly in the brightness and contrast of the finger vein images. The thickness of the finger impacts the overall amount of light that penetrates the tissue, influencing the image's brightness. Additionally, variations in tissue density affect how light scatters within the finger, leading to differences in image contrast. Understanding and harnessing these inherent characteristics play a pivotal role in our finger vein recognition model, as they contribute to the rich tapestry of soft biometric traits we use for accurate and reliable user identification. By considering these nuanced aspects, our system excels in discerning individuals even amidst the intricacies of real-world scenarios, making it a robust choice for biometric authentication.

Let (x, y) be the background layer image, and w and h be the width and the height of the image, respectively.

$$M = \frac{\sum_{i=1}^{wh} I_i(x, y)}{wh} \quad (1)$$

The variance V is:

$$V = \frac{\sum_{i=1}^{wh} (I_i(x, y) - M)^2}{wh} \quad (2)$$

$$f_1 = [M, V] \quad (3)$$

3.3.4 Array of Mean and Variance

Individuals exhibit varying knuckle width and finger length, leading to distinct spatial characteristics in the bright and dark regions of finger vein images. These unique physical attributes influence how light interacts with the finger's surface, resulting in diverse patterns of brightness and contrast. Recognizing and leveraging these inherent differences is essential in our finger vein recognition system. By considering these spatial properties, our model excels in accurately distinguishing individuals, offering a robust and effective means of biometric authentication, even in complex real-world scenarios.

Variations in individuals' knuckle width and finger length lead to distinct spatial characteristics in both the bright and dark regions. To capture these unique traits, we partition the background layer image into $a \times b$ blocks. Within each of these blocks, we calculate the grayscale mean (m) and grayscale variance (v), denoted by v ($1 \leq i \leq a \times b$). These values are then concatenated to form a $2 \times a \times b$ -dimensional soft biometric trait known as the "Array of Mean and Variance" (AM&V). This trait encapsulates the nuanced information about the mean and variance of intensity distribution across the image blocks, offering a comprehensive representation of the spatial properties within the background layer image for accurate individual characterization.

$$f_2 = [m_1, v_1] (1 \leq ia \times b) \quad (4)$$

3.3.5. Local Binary Pattern

Local Binary Pattern (LBP) relies on four essential parameters for its operation:

Radius: The radius defines the extent of the circular region around the central pixel when constructing the local binary pattern. Typically, it is set to 1, but it can be adjusted to influence the pattern's sensitivity to local variations.

Neighbors: The number of neighboring sample points considered when building the circular local binary pattern. It's important to note that increasing the number of sample points also increases the computational workload. Usually, it's set to 8, but you can adjust it depending on the desired level of detail and computational resources available.

Grid X: This parameter denotes the number of cells in the horizontal direction when dividing the image into a grid for feature extraction. A higher value creates a finer grid, resulting in a feature vector with higher dimensionality. It's commonly set to 8, but you can modify it based on the granularity required for your application.

Grid Y: Similar to Grid X, Grid Y specifies the number of cells in the vertical direction when dividing the image into a grid. Adjusting this value can influence the granularity of the feature vector. Typically, it's also set to 8, but it can be tailored to suit specific feature extraction needs.

These parameters allow to fine-tune the LBP algorithm to balance computational efficiency and the level of detail captured in the resulting feature vectors, making it adaptable for image analysis tasks.

3.3.6. Histogram of Spatial Pyramid

The extraction of soft biometric traits, such as Mean & Variance and Array of Mean & Variance, is traditionally conducted at a single scale, but to capture a more comprehensive understanding of finger vein patterns, we employ a sophisticated multiscale approach. In this method, we utilize a spatial pyramid to partition the finger vein image into sub-images at two different scales. Within each of these sub-images, we meticulously calculate gray scale histograms.

This meticulous process results in what we term the "Histogram of Spatial Pyramid" (HSP). HSP encapsulates the combined information from these histograms in each sub-image block, effectively creating a holistic representation of the intricate spatial characteristics of finger vein patterns across multiple scales. This multiscale feature construction not only enhances the richness of our soft biometric traits but also reinforces the robustness of our finger vein recognition model, ensuring accurate user identification in a wide range of scenarios, even when confronted with varying spatial properties within the finger vein images.

3.4 CLASSIFICATION

A Convolutional Neural Network (CNN) is a powerful architecture composed of interconnected layers, where each layer transforms one data volume into another using differentiable function. Within the CNN framework, there exists a diverse array of layer types, each serving a specific purpose in the network's operations.

When constructing a CNN model, we typically take input images, such as one with dimensions of 320x240 pixels. These images undergo a series of convolutional operations, pooling layers, and nonlinear activation functions. Convolutional layers specialize in feature extraction, while pooling layers reduce spatial dimensions, and activation functions introduce nonlinearity, enhancing the model's capacity to capture complex patterns and hierarchical representations within the input data.

By systematically processing and transforming the input image through these layers, the CNN learns to extract meaningful features and representations, ultimately enabling it to perform tasks like image classification, object detection, and more. This ability to automatically learn and adapt to various visual patterns makes CNNs a cornerstone in the realm of computer vision and deep learning.

3.4.1 Information Layer

This particular layer in the neural network architecture serves as a crucial repository for the unprocessed, raw contributions of an input image with dimensions of 320 pixels in width and 240 pixels in height. At this initial stage, the layer retains the pixel-level information, preserving the intricate details and color values present in the image.

3.4.2 Convolution Layer

This particular layer plays a pivotal role in the neural network's operations, as it computes the output volume by performing a dot product operation between every channel in its input and a fixed image patch. This process is a fundamental step in feature extraction and transformation within the network. Here, each channel represents a distinct aspect or feature of the input data, and the dot product with the fixed image patch allows the layer to capture correlations, relationships, and patterns between these features and the designated patch. This operation effectively highlights the significance of different parts of the input data and enables the network to discern relevant information for subsequent processing.

By systematically performing these dot product computations across all channels, this layer contributes to building a rich and informative output volume, facilitating the network's ability to recognize complex patterns, make informed decisions, and ultimately excel in tasks like image recognition, object detection, and more.

3.4.3 Actuation Function Layer

The Activation Function Layer is a pivotal component within a neural network, tasked with applying various activation functions to the output of preceding layers, such as the convolutional layer. These functions introduce essential nonlinearity into the network, enabling it to capture intricate relationships and extract informative features from the data. Common activation functions include ReLU, Sigmoid, Tanh, Leaky ReLU, and more. The choice of activation function has a substantial impact on a network's learning capacity and performance, making it a critical aspect of neural network design.

3.4.4 Pooling Layer

Within the architecture of convolutional neural networks (CNNs), there exists a critical layer known as the pooling layer, periodically interspersed throughout the network. Its primary purpose is to systematically reduce the spatial dimensions of the data volume. This reduction serves multiple vital functions: it accelerates computational processing, conserves memory resources, and serves as a regularization technique, helping prevent over fitting.

There are two prevalent types of pooling layers commonly used in CNNs: max pooling and average pooling. These layers play a pivotal role in feature extraction within a CNN. Initially, the network extracts features by convolving the input data with a set of kernel filters. Subsequently, the pooling operation is applied to the obtained features. This pooling process effectively condenses the information and passes it to the subsequent layers, contributing to the network's ability to learn hierarchical representations and recognize complex patterns within the data.

$$x_i^l \in R^{M_i * M_l} \tag{5}$$

The provided equation represents the I^{th} layer of the i^{th} map, where the kernel filter of the I^{th} layer is connected to the i^{th} map in the $(l - 1)^{th}$ layer, along with an associated index map.

$$x_i^l = f \left(\sum_{i \in M_j} X_i^{l-1} * k_{ij}^l + b_j^l \right) \tag{6}$$

The equation shown represents the convolution operation, with 'f(.)' denoting the activation function, commonly referred to as ReLU (Rectified Linear Unit), defined as $f(z) = \max(0, z)$. Following this, the pooling operation can be expressed as follows:

$$x_i^l = \text{down} (x_i^{l-1}) \tag{7}$$

Where $\text{down}(\cdot)$ is represented as sum-sampling function.

In the implementation of the residual network, the architecture is thoughtfully designed to incorporate distinct changes in layers at each step. This design not only outlines the structural modifications but also provides insights into the network's performance and the time it takes at each execution stage. This system comprises five convolutional stages, and it is pre-trained on a dataset derived from the Large-Scale Visual Recognition Challenge (ILSVRC) 2015 test. The primary goal of this test dataset is to facilitate the recognition of intricate features in finger vein images and categorize objects depicted in photographs. This comprehensive dataset encompasses a total of 1000 distinct classes for classification purposes.

Interestingly, although the system is initially pre-trained on scenes and object images, preliminary analyses reveal its superior performance when compared to a ResNet-18 model pre-trained on texture-based images. This result is somewhat surprising since the visual characteristics of textures closely resemble those in finger vein detection images. Despite this resemblance, the network's performance is significantly worse when leveraged in the texture domain, highlighting the complexity of recognizing scenes and objects compared to simple surface textures. As such, the system fine-tuned to perceive scenes and objects excels at identifying unexpected and intricate patterns within finger vein detection images. The proposed system's flow diagram is depicted in Figure 2.

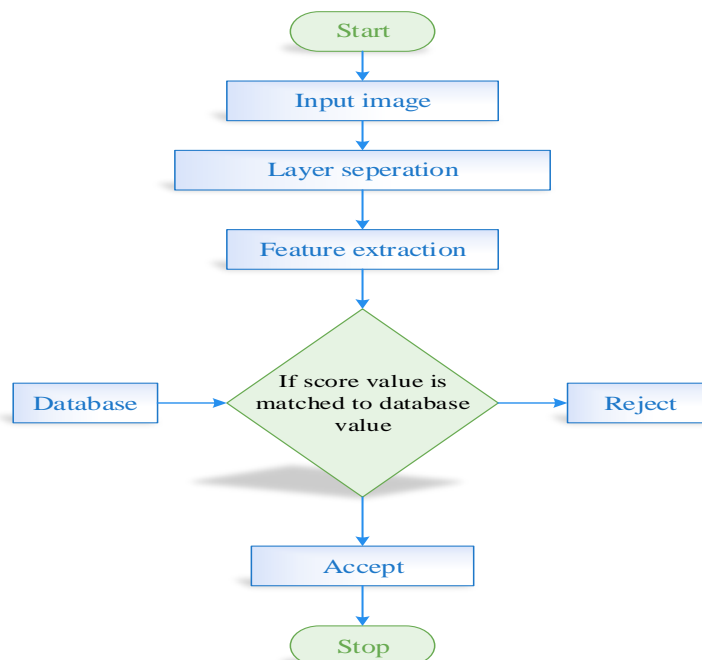


Figure.2. Flow Diagram of Proposed System

Initiating the process with an input image, specifically a finger vein image, the system employs a layer separation technique to discern and isolate crucial components within the foreground and background layers. Feature extraction methods are then utilized to capture both primary and soft biometric traits for identification purposes. The extracted features undergo comparison with entries in the database, and if the score value aligns with a database value, the system makes a decision to either accept or reject the input.

IV. RESULT AND DISCUSSION

4.1 INPUT IMAGE

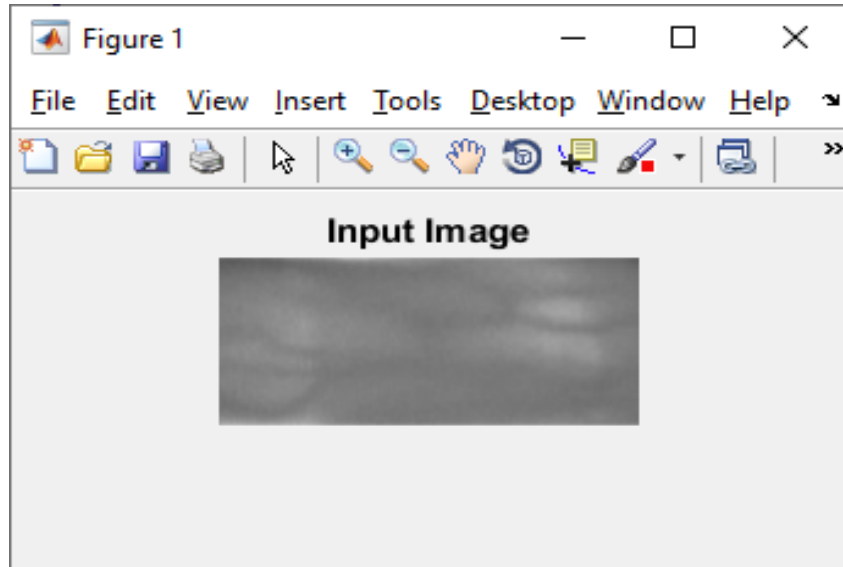


Figure.3. Input Image

The process begins with the selection of an input image file through the utilization of the 'uigetfile' command, enabling user interaction for file selection. Following this selection, the chosen input image, which typically adheres to the .bmp format, is then read into the program using the 'imread' command. This pivotal step in the image processing pipeline serves as the gateway to access and manipulate the image's pixel data for further analysis, enhancement, or feature extraction.

4.2 RESIZE IMAGE

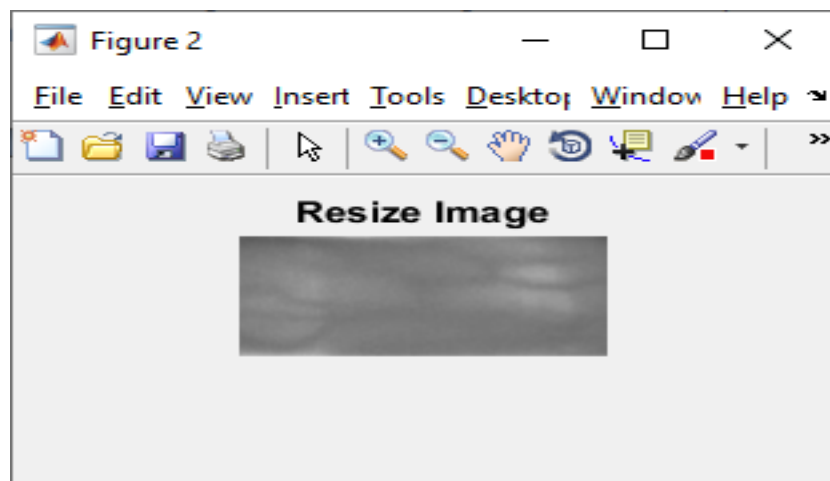


Figure.4. Resize Image

To prepare the input image for further processing, the 'imresize' function is employed to resize it. Specifically, the size adjustment is set to a scale factor of 0.80. This resizing operation ensures that the image is brought to a desired scale, making it suitable for subsequent tasks such as feature extraction, analysis, and display.

In this case, the scale factor of 0.80 indicates that the image is reduced to 80% of its original dimensions, potentially improving processing efficiency or fitting the image into a predetermined layout or template. This

resizing step plays a crucial role in the image processing pipeline, facilitating seamless integration with subsequent operations.

4.3 GRAY IMAGE

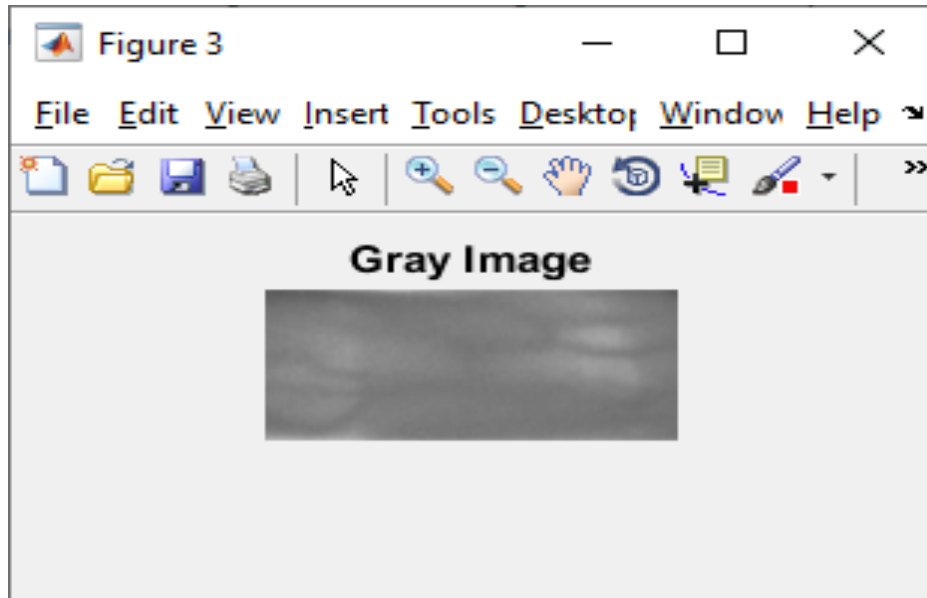


Figure.5. Gray Image

Following the resizing operation, the next step involves transforming the input image into grayscale format, a monochromatic representation commonly used in image processing. To achieve this conversion, the 'rgb2gray' function is employed. Grayscale images, unlike their RGB counterparts, contain only intensity information, simplifying subsequent analysis and reducing computational overhead. In the grayscale format, pixel values range from 0 (black) to 1 (white), representing varying levels of brightness and contrast within the image. This conversion not only reduces the dimensionality of the data but also enhances the focus on critical image details. By displaying the image in this black and white format, we establish a clear visual representation where black pixels correspond to the value 0 and white pixels correspond to the value 1. This binary interpretation simplifies thresholding, edge detection, and other image processing operations, making it an integral step in preparing the image for further analysis or visualization.

4.4 HISTOGRAM EQUALIZATION

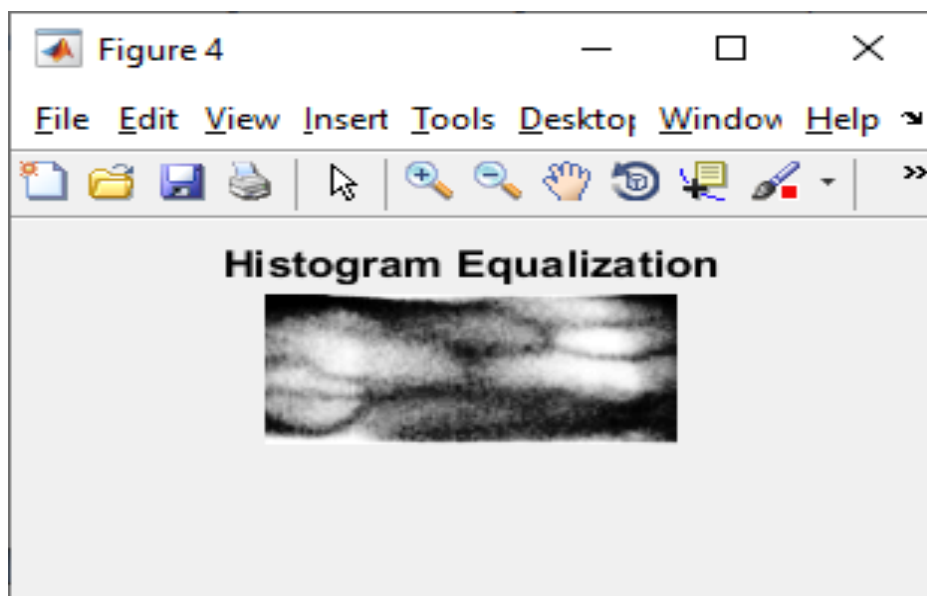


Figure.6. Histogram Equalization

Histogram equalization is employed to adjust the intensity values of gray scale images. In this process, the 'histeq' function is applied to the image and redistributes the pixel intensity values across the entire spectrum by maximizing the image's contrast and improving its visual quality.

4.5 IMAGE LAYER SEPARATION

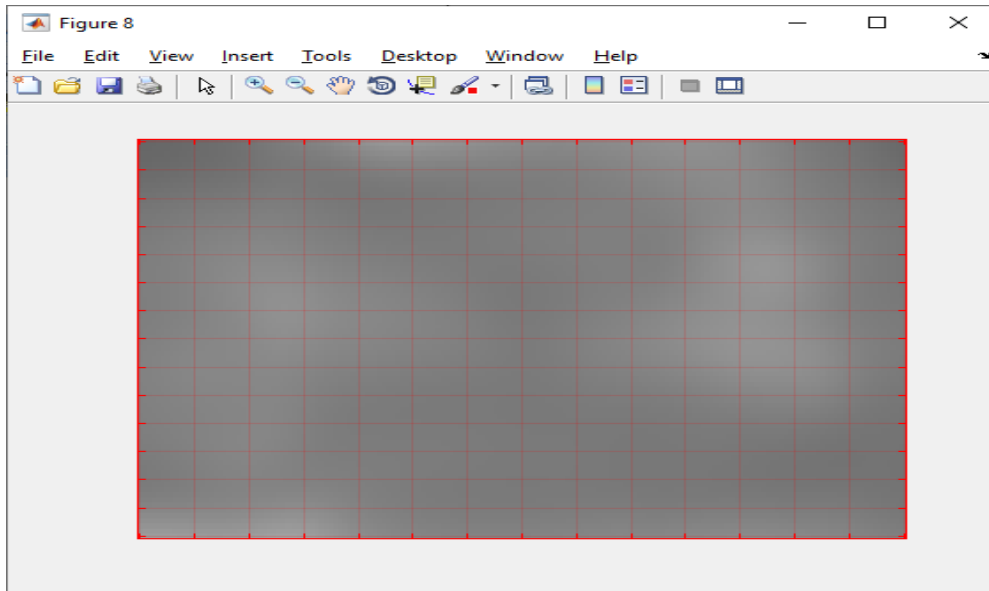


Figure.7. Image Layer Separation

Image layer separation (ILS) is a type of algorithm that separates an image into a smooth layer and a high-gradient layer, which is commonly used for intrinsic image decomposition and single-image reflection interference removal.

4.6 FOREGROUND LAYER AND MAIN FEATURE

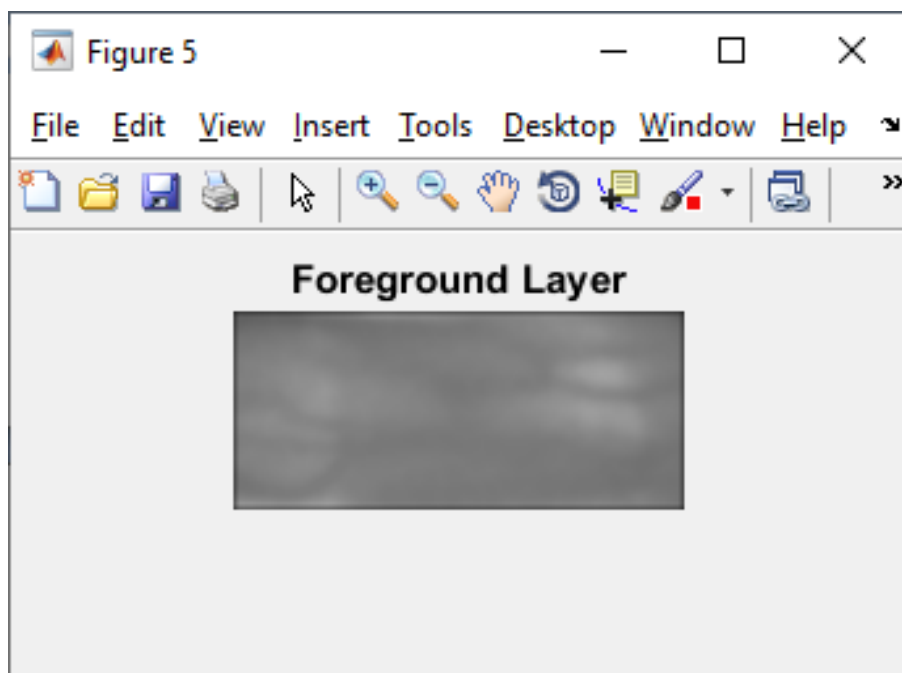


Figure.8. Foreground Layer

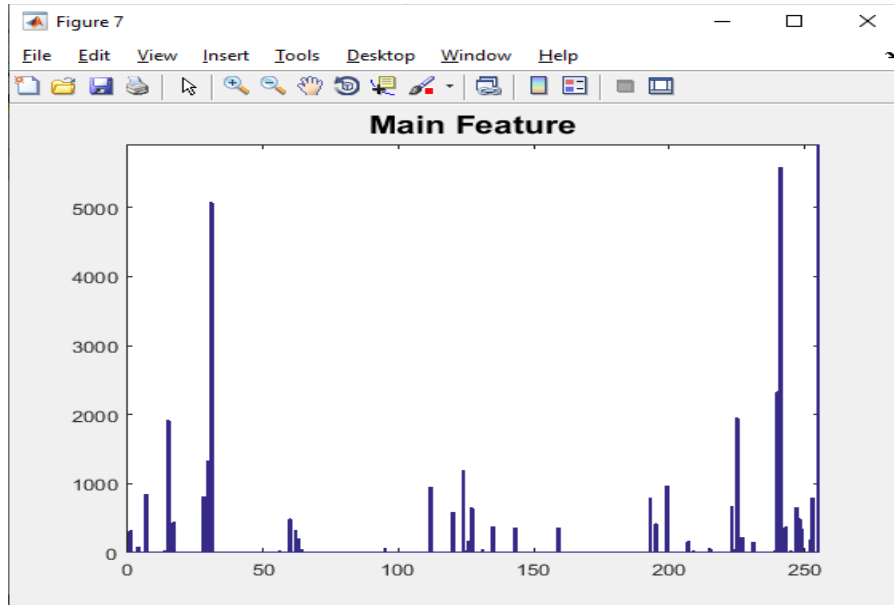


Figure.9. Main Feature

LBP is an efficient texture extraction algorithm with illumination and rotation invariance, which is usually applied to face recognition and vein recognition. The main idea of LBP is to measure the gray change between each pixel and its neighborhood and to code this change to generate the LBP code histogram, which can fully represent the finger vein feature but cannot handle the texture transition.

4.7 BACKGROUND LAYER AND SOFT FEATURE

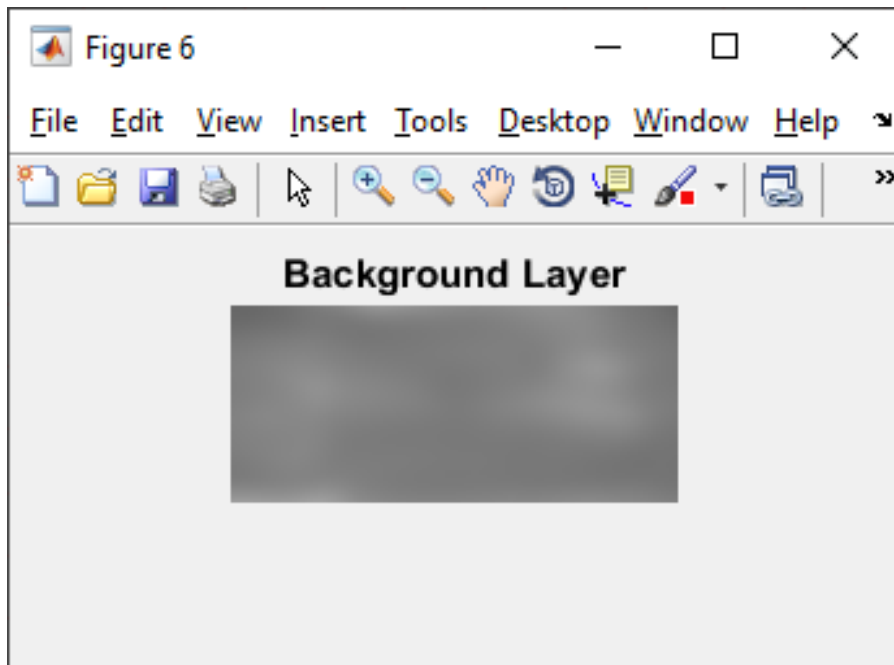


Figure.10. Background Layer

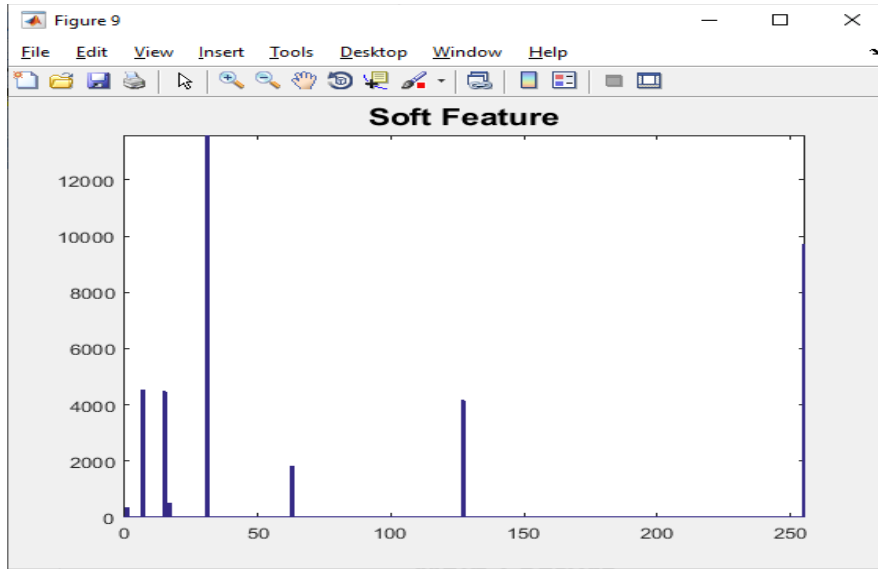
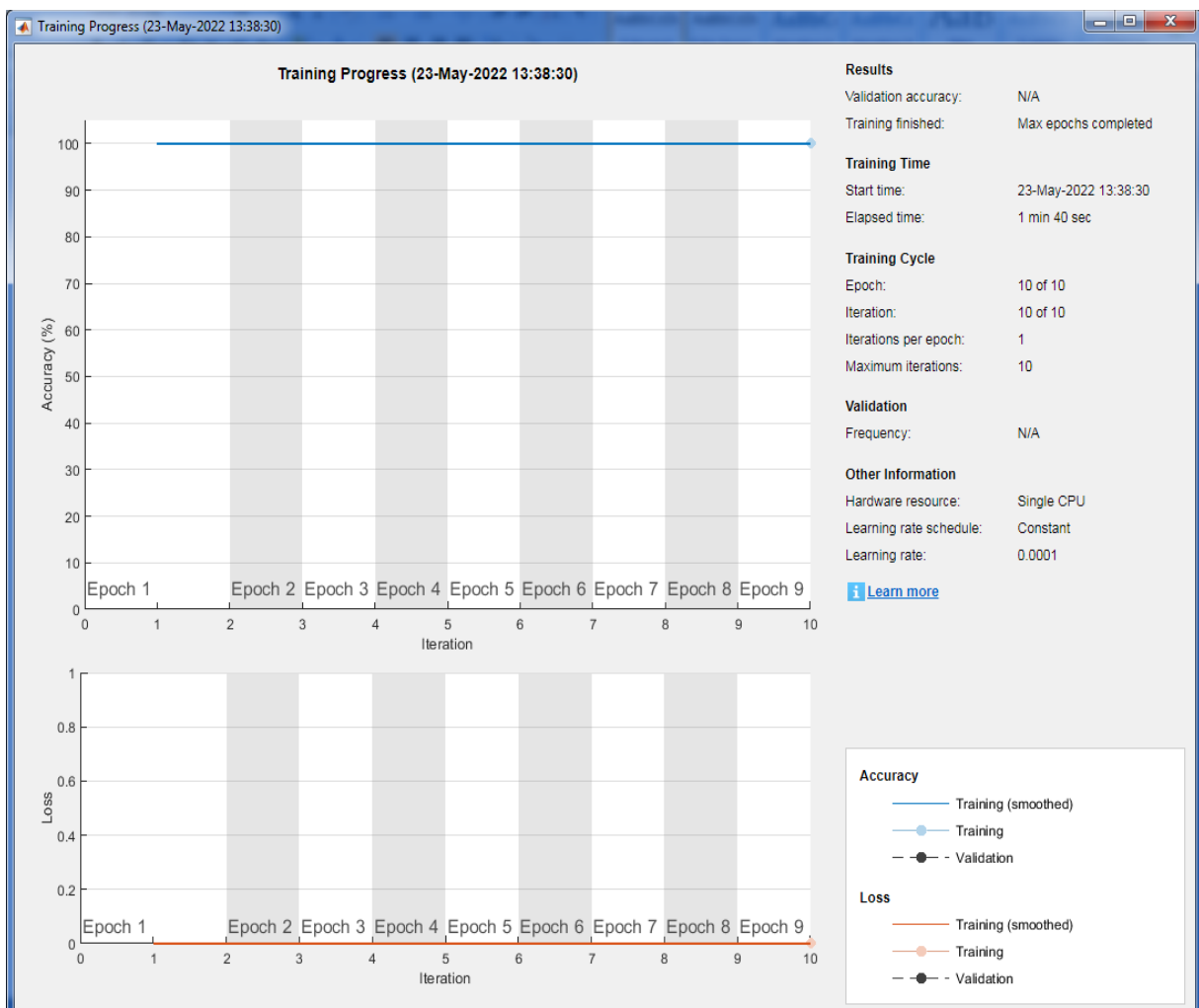


Figure.11. Soft Feature

A background layer is the intensity distribution. For this characteristic, we design three kinds of soft biometric traits that are extracted from the background layer, i.e., the mean and variance, the array of mean and variance, and the histogram of spatial pyramid.

4.8 CNNRESNET CLASSIFIER



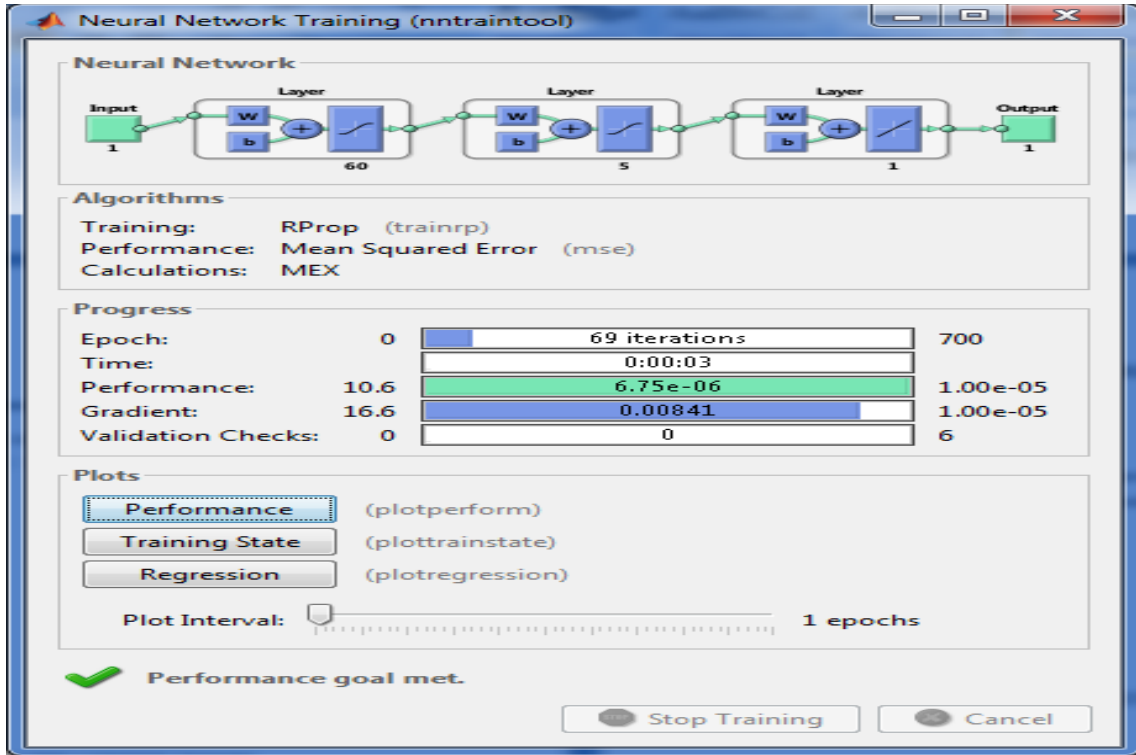


Figure.12. CNNResNet Classifier

The diagram above illustrates the CNNResNet Trainer Tool, comprising distinct sections: the input layer, three hidden layers, and the output layer. This tool plays a pivotal role in training convolutional neural networks (CNNs) with the ResNet architecture. The input layer accepts data, while the three hidden layers process and extract features. Finally, the output layer generates predictions or classifications.

4.9 AUTHENTICATION DIALOGUE BOX

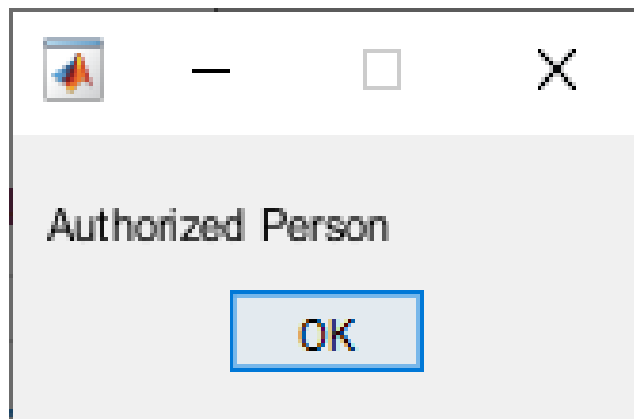


Figure.13. Authentication dialogue box

The displayed dialogue box conveys that the input image has successfully matched with a record in the database, suggesting a positive identification or recognition result.

V. CONCLUSION

Historically, finger vein recognition research primarily focused on texture features while overlooking the significance of intensity distribution in the background, often dismissing it as noise. However, this paper introduces a comprehensive approach, analyzing finger vein imaging theory and image features, and proposing a soft biometric trait extraction algorithm. Initially, the background layer, excluding finger vein texture, is extracted using ILS and GB methods. Subsequently, the intensity distribution within the background layer is characterized through three soft biometric traits. To enhance matching accuracy, a CNNRESNET 18 model is

introduced, yielding an impressive accuracy rate of 99.98%. Notably, the experimental results reveal that GB, while less time-consuming than ILS, achieves comparable performance. Future research avenues may explore classifier types to enhance retinal recognition, with a focus on employing Neuro-fuzzy techniques to reduce training time. Leveraging soft-computing techniques like fuzzy systems for automatic retinal identification yields superior results compared to manual approaches. Ongoing work will aim to further understand image method characteristics for enhanced Sensitivity, specificity, and Accuracy values.

VI. REFERENCE

- [1] S.-C. Wu, P.-L. Hung, and A. L. Swindlehurst, "ECG biometric recognition: Unlinkability, irreversibility, and security," *IEEE Internet Things J.*, vol. 8, no. 1, pp. 487–500, Jan. 2021.
- [2] G. Jack, M. Ji, and C. Danny, "Matching larger image areas for unconstrained face identification," *IEEE Trans. Cybern.*, vol. 49, no. 8, pp. 3191–3202, Aug. 2019.
- [3] A. Sengupta and M. Rathor, "Securing hardware accelerators for CE systems using biometric fingerprinting," *IEEE Trans. Very Large Scale Integr. (VLSI) Syst.*, vol. 28, no. 9, pp. 1979–1992, Sep. 2020.
- [4] X. Qian, Y. Fu, T. Xiang, Y.-G. Jiang, and X. Xue, "Leader-based multi-scale attention deep architecture for person re-identification," *IEEE Trans. Pattern Anal. Mach. Intell.*, vol. 42, no. 2, pp. 371–385, Feb. 2020.
- [5] Yang, W., Hui, C., Chen, Z., Xue, J.H. and Liao, Q., 2019. FV-GAN: Finger vein representation using generative adversarial networks. *IEEE Transactions on Information Forensics and Security*, 14(9), pp.2512-2524.
- [6] W. Yang, S. Wang, J. Hu, G. Zheng, J. Yang, and C. Valli, "Securing deep learning based edge finger vein biometrics with binary decision diagram," *IEEE Trans. Ind. Informat.*, vol. 15, no. 7, pp. 4244–4253, Jul. 2019.
- [7] W. Yang, W. Luo, W. Kang, Z. Huang, and Q. Wu, "FVRAS-net: An embedded finger-vein recognition and AntiSpoofing system using a unified CNN," *IEEE Trans. Instrum. Meas.*, vol. 69, no. 11, pp. 8690–8701, Nov. 2020.
- [8] R. S. Kuzu, E. Piciucco, E. Maiorana, and P. Campisi, "On-the-fly fingervein-based biometric recognition using deep neural networks," *IEEE Trans. Inf. Forensics Security*, vol. 15, pp. 2641–2654, 2020.
- [9] W. Kang, H. Liu, W. Luo, and F. Deng, "Study of a full-view 3D finger vein verification technique," *IEEE Trans. Inf. Forensics*, vol. 15, pp. 1175–1189, 2020.
- [10] J. Zhang, Z. Lu, and M. Li, "Active contour-based method for fingervein image segmentation," *IEEE Trans. Instrum. Meas.*, vol. 69, no. 11, pp. 8656–8665, Nov. 2020.
- [11] W. Kang, Y. Lu, D. Li, and W. Jia, "From noise to feature: Exploiting intensity distribution as a novel soft biometric trait for finger vein recognition," *IEEE Trans. Inf. Forensics Security*, vol. 14, no. 4, pp. 858–869, Apr. 2019.
- [12] R. Ramachandra, K. B. Raja, S. K. Venkatesh, and C. Busch, "Design and development of low-cost sensor to capture ventral and dorsal finger vein for biometric authentication," *IEEE Sensors J.*, vol. 19, no. 15, pp. 6102–6111, Aug. 2019.
- [13] A. Banerjee, S. Basu, S. Basu, and M. Nasipuri, "ARTeM: A new system for human authentication using finger vein images," *Multimedia Tools Appl.*, vol. 77, no. 5, pp. 5857–5884, Mar. 2018.
- [14] H. Liu, G. Yang, and Y. Yin, "Category-preserving binary feature learning and binary codebook learning for finger vein recognition," *Int. J. Mach. Learn. Cybern.*, vol. 11, no. 11, pp. 2573–2586, Jun. 2020.
- [15] W. Hussain, N. Rasool, and M. Yaseen, "ADVIT: Using the potentials of deep representations incorporated with grid-based features of dorsum vein patterns for human identification," *Forensic Sci. Int.*, vol. 313, Aug. 2020, Art. no. 110345.
- [16] W. Yang, C. Hui, Z. Chen, J.-H. Xue, and Q. Liao, "FV-GAN: Finger vein representation using generative adversarial networks," *IEEE Trans. Inf. Forensics Security*, vol. 14, no. 9, pp. 2512–2524, Sep. 2019.
- [17] R. S. Kuzu, E. Maiorana, and P. Campisi, "Vein-based biometric verification using densely-connected convolutional autoencoder," *IEEE Signal Process. Lett.*, vol. 27, pp. 1869–1873, 2020.
- [18] R. He, J. Cao, L. Song, Z. Sun, and T. Tan, "Adversarial cross-spectral face completion for NIR-VIS face recognition," *IEEE Trans. Pattern Anal. Mach. Intell.*, vol. 42, no. 5, pp. 1025–1037, May 2020.

- [19] R. He, X. Wu, Z. Sun, and T. Tan, "Wasserstein CNN: Learning invariant features for NIR-VIS face recognition," IEEE Trans. Pattern Anal. Mach. Intell., vol. 41, no. 7, pp. 1761–1773, Jul. 2019.
- [20] J. Zeng et al., "Finger vein verification algorithm based on fully convolutional neural network and conditional random field," IEEE Access, vol. 8, pp. 65402– 65419, 2020.
- [21] J. Zeng et al., "Real-time segmentation method of lightweight network for finger vein using embedded terminal technique," IEEE Access, vol. 9, pp. 303–316, 2021.
- [22] K. Wang, G. Chen, and H. Chu, "Finger vein recognition based on multi- receptive field bilinear convolutional neural network," IEEE Signal Process. Lett., vol. 28, pp. 1590–1594, 2021.